

Directional Threading and Sliding of a Dissymmetrical Foldamer Helix on Dissymmetrical Axles

Xiang Wang, Quan Gan, Barbara Wicher, Yann Ferrand,* and Ivan Huc*

Abstract: We have investigated the self-assembly of a dissymmetrical aromatic oligoamide helix on linear amido-carbamate rods. A dissymmetric sequence bearing two differentiated ends is able to wrap around dissymmetric dumbbell guest molecules. Structural and thermodynamic investigations allowed us to decipher the mode of binding of the helix that can bind specifically to the amide and carbamate groups of the rod. In parallel kinetic studies of threading and sliding of the helix along linear axles were also monitored by ^1H NMR. Results show that threading of a dissymmetrical host can be kinetically biased by the nature of the guest terminus allowing a preferential sense of sliding of the helix. The study presented below further demonstrates the valuable potential of foldaxanes to combine designed molecular recognition patterns with fine control of self-assembly kinetics to conceive complex supra-molecular events.

Inspired by the molecular biomachinery, chemists have long tried to reproduce the controlled directional translations observed, for example, in the motion of DNA polymerases along DNA templates or of kinesin proteins along microtubules. Abundant literature thus exists on the translation of macrocycles on rod-like molecular axles.^[1] Miniature artificial walkers have also been described.^[2,3] Translation directionality can be imposed when changing the preferred position of macrocycles on a molecular rod by means of an external stimulus. Biased Brownian motion then allows the system to relax to its new preferred state leading to a net flux from one station to the other.^[4] Reverting the preferred position back to its original state leads to a reversal of translation and shuttling is observed.^[5] Besides the directionality of the motion, the relative inherent orientation of the axle and the component that slides along it is an intriguing aspect that has

less often been addressed.^[6–8] This stems from the fact that most macrocycles that have been used as molecular shuttles have a symmetrical structure. In contrast dissymmetrical macrocycles, for example, cone-shaped calixarenes^[6] cyclodextrins^[7] and others,^[8] may thread onto a dissymmetrical axle. The lack of symmetry allows for the definition of a front and a rear of the shuttle, and also of forward and backward motions. By extension, one could imagine chemical transformations that would occur exclusively at the rear and favor forward motion, for example via a ratcheting mechanism induced by processive catalysis (i.e., the installation of stoppers on the rod), or via a self-propelling mechanism.^[9] As preliminary steps towards this goal, we herein present a dissymmetrical helix-rod host-guest system with a very strong thermodynamic preference for a particular relative helix/rod orientation (Figure 1 a). We also show that kinetic bias in threading the rod into the helix cavity allows for the implementation of the directional motion of an oriented helix along an oriented rod.

We have previously introduced multi-turn helical aromatic oligoamide foldamers that form stable pseudo-rotaxane complexes, also termed foldaxanes, around rod-like guests.^[10,11] Helices based on 7-amino-8-fluoro-2-quinoline-carboxylic acid oligoamides such as **1** possess a tubular cavity that can accommodate α,ω -alkanediamine-derived dicarbamate guests and slide along them. Threading and sliding of these helices along guests are much faster than their direct unwinding and rewinding, allowing for the design of kinetically favored supramolecular pathways depending on whether bulk too large to pass through the helix cavity is on the way or not.^[12] Solution and solid state data demonstrated that helix-rod association is mainly driven by hydrogen bonds between carbamate carbonyl groups on the rods and 2,6-pyridinedicarboxamide protons on the helix carbamate cleft (CC in Figure 1 b). This interaction should in principle make it possible to bind rods with other carbonyl-containing groups than carbamates. However, oligomers such as **1** do not bind to diamide rods or to α,ω -alkanediol-derived dicarbamate rods, that is, when the orientation of the carbamates has been reverted. A closer look at earlier crystal structures^[11a] pointed to secondary hydrogen bonding between the terminal pivaloyl amide proton and the carbamate sp³ oxygen atom as being responsible for this selectivity (Figure 1 c). This observation hinted at the possibility to replace the foldamer terminal amide NH donor by a hydrogen acceptor and change guest selectivity, eventually giving access to dissymmetrical guest binding.

The amide cleft (AC) segment was designed for this purpose (Figure 1 b). For this, the terminal pyridine ring of CC was mutated into a naphthyridine^[13] unit with the hope to

[*] X. Wang, Q. Gan, Dr. Y. Ferrand, Prof. I. Huc
CBMN (UMR5248), Univ. Bordeaux—CNRS—IPB
Institut Européen de Chimie et Biologie
2 rue Escarpit, 33600 Pessac (France)
E-mail: y.ferrand@iecb.u-bordeaux.fr

Dr. B. Wicher

Department of Chemical Technology of Drugs
Poznan University of Medical Sciences
Grunwaldzka 6, 60–780 Poznan (Poland)

Prof. I. Huc

Department Pharmazie and Center for Integrated Protein Science
Ludwig-Maximilians-Universität
Butenandtstrasse 5–13, 81377 München (Germany)
E-mail: ivan.huc@cup.lmu.de

Supporting information and the ORCID identification number(s) for the author(s) of this article can be found under:
<https://doi.org/10.1002/anie.201813125>.

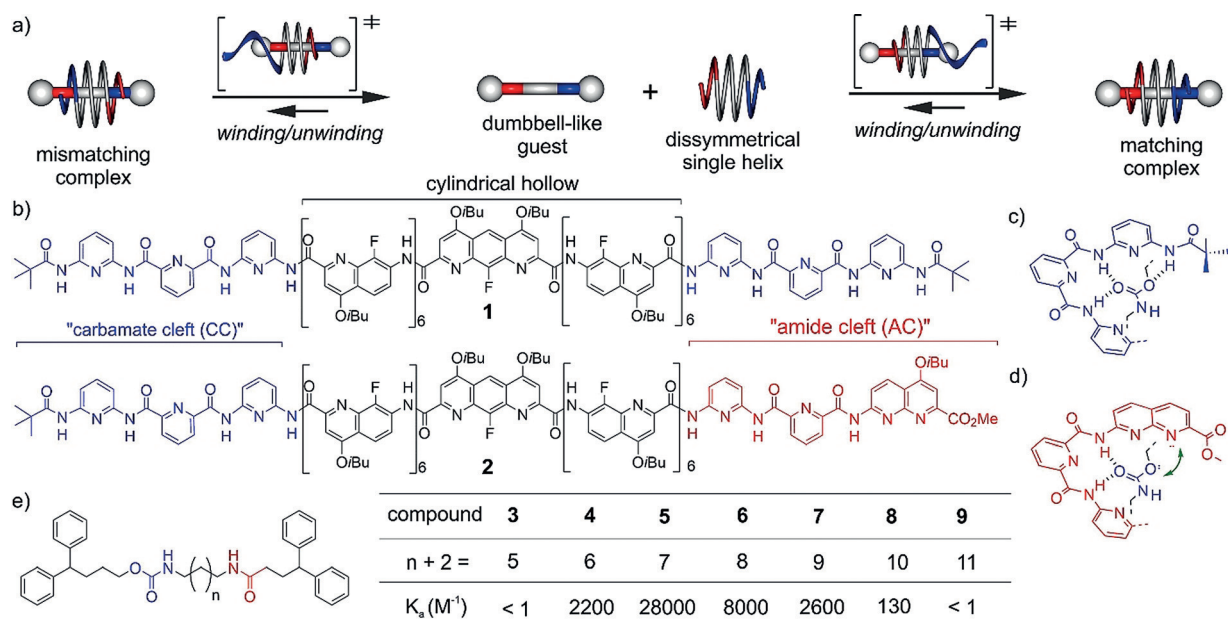


Figure 1. Host-guest components and assembly. a) Schematic representation of the complex formation between a dissymmetric single helix and a dissymmetric dumbbell guest. b) Formula of **1** and **2**. Binding mode of a carbamate in a carbamate cleft (blue, c) or in an amide cleft (red, d). The latter is destabilized by electrostatic repulsion (green double arrow). e) Formula of dumbbell guests **3–9** and their association constants (K_a) with **2** at 323 K.

create repulsive electrostatic interactions with the carbamate sp³ oxygen atom of the rod (Figure 1d). By analogy with **1**, sequence **2** comprising a CC and an AC terminal segments was thus designed and synthesized (see the supporting information). To ascertain our hypothesis, dumbbell shaped guests **3–9** including both amide and carbamate groups were also prepared (Figure 1e). Titrations between single helix **2** and rods **3–9** were monitored by ¹H NMR in CDCl₃ and, in some cases, revealed the emergence of a single new species in slow exchange on the NMR time scale typical of foldaxane formation (Figures S12–S17 in the Supporting Information). As previously observed for binding studies between **1** and dicarbamate rods,^[14] high foldaxane stability with **2** requires a match between the helix and the rod lengths (Figure 1e). The highest affinity constant was obtained for rod **5** bearing seven methylene units between its two binding anchors ($K_a = 2.8 \times 10^4 M^{-1}$).

Because of the dumbbell shape of the guests, host-guest complex formation with **3–9** requires the winding of the helix around the rod and this process is slow (Figure 1a). Monitoring of the binding of **5** by **2** at 323 K (i.e., under slight heating) revealed the progressive disappearance of the empty host, the concomitant emergence of the thermodynamically favored complex and also the transient appearance of another species (Figure 2a–d). This is consistent with the initial formation of both a matching and a mismatching complex followed by the progressive disappearance of the less stable mismatching complex. At equilibrium, the minor species has disappeared showing quantitative bias as far as NMR can detect. Remarkably, the initial proportion of the mismatching complex is small (less than 6%), indicating that this species is not only less stable, in other words that it has a larger dissociation rate constant, but also that it has a slower formation rate.

Thus, upon winding around the rod, the helix finds a faster pathway towards the most stable complex.

Structural information on **2**⊃**5** and in particular its assignment to a matching complex was gathered using X-ray crystallography. Single crystals were obtained by slow diffusion of *n*-hexane into a chloroform solution. The structure revealed that the single helix can fully wrap around the alkyl segment of the rod whose diphenyl groups protrude from both apertures of the foldamer cavity (Figure 2e,f). The structure fully validates the initial hypothesis that the newly designed AC binds to the amide group whereas the CC hydrogen bonds to the carbamate of the guest (Figure 2g,h). These favorable interactions and the repulsions that are expected to occur in the mismatching complex are strong enough to achieve quantitative selectivity in solution.

Foldaxane formation was then investigated with single station rods **10** and **11** possessing a bulky stopper at one end only (Figure 3a). This design allows for the unhindered threading of the other end of each axle into the helix at rates much faster than the winding of the helix onto binding stations (Figure 3b). Threading is actually so fast that an oligoethylene glycol chain (PEG750, M.W. = 750 g mol⁻¹) had to be introduced and the samples cooled to 273 K to slow it down and observe intermediates before equilibrium is reached. Rods **10** and **11** were used to study a possible preferred direction of threading. They both have a methoxy-terminated PEG chain and differ mainly in the position of amide and carbamate groups: the respective matching and mismatching complexes on these two rods have opposite orientations. For both rods, the two complexes are easily distinguished by ¹H NMR. In the case of **10**, some mismatching complex was detected but, even at very early stages of the threading, its proportion remained small (<20%). At equi-

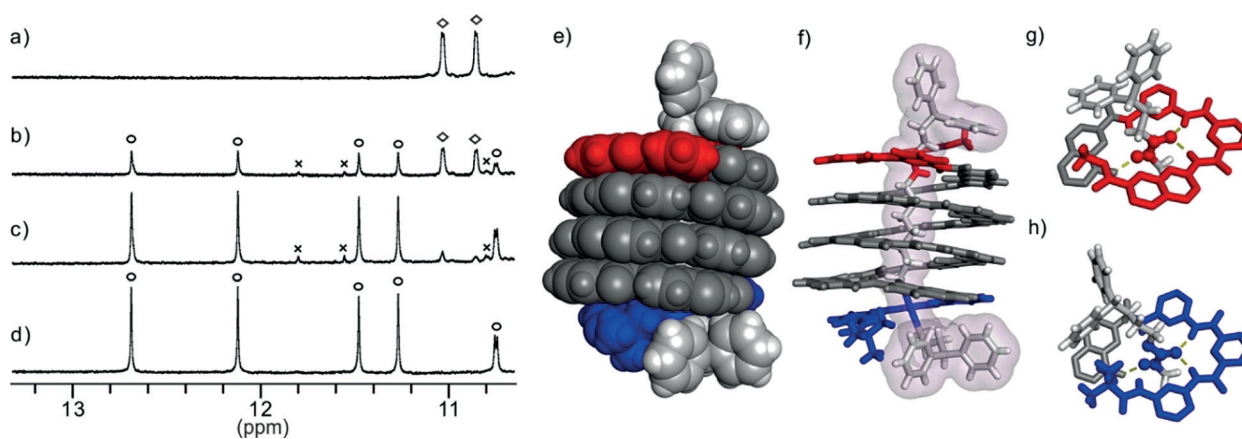


Figure 2. Excerpts of 400 MHz ¹H NMR spectra (323 K in CDCl₃) showing the amide resonances of **2** at 1 mM (a) and in the presence of 3 equiv of **5** after: b) 5 min; c) 60 min. and d) at equilibrium. Amide signals of the free single helix **2**, matching and mismatching complexes **2**⊃**5** are marked with empty diamonds, empty circles and black crosses, respectively. e, f) Side views of **2**⊃**5** solid state structure analyzed by single crystal X-ray crystallography. In (e) the helix and the dumbbell rod are shown in CPK representation. In (f) the helix and the rod are shown as tube representation. The latter is covered by a transparent isosurface representing its volume. g, h) Views from above and below showing the binding modes between AC and CC and the amide and carbamate groups of the rods shown in red and blue colors, respectively. In (e–h) CC and AC and the central helical segment are colored in blue, red and grey, respectively. Side chains (OiBu groups) and included solvent molecules have been removed for clarity.

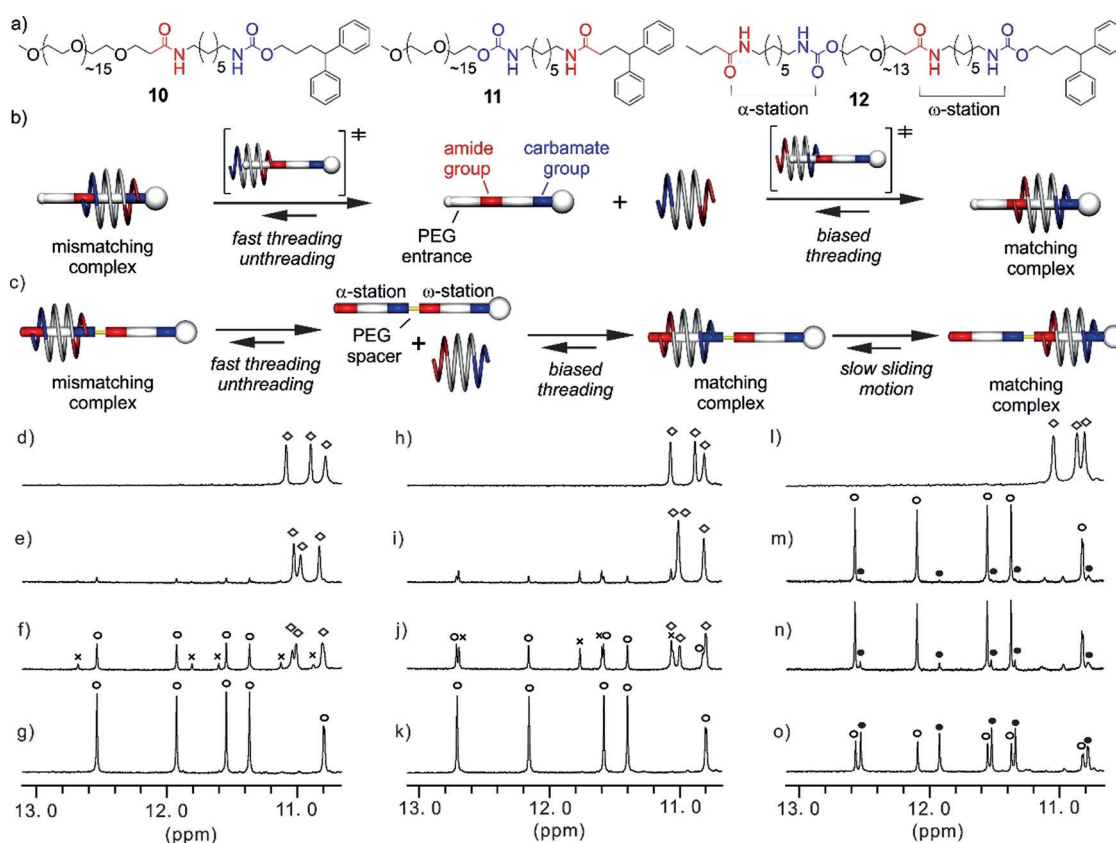


Figure 3. a) Formula of rods **10**–**12**. Schematic representations of: b) the biased threading of a dissymmetrical single helix along a dissymmetrical rod and c) the threading followed by the unidirectional sliding of a dissymmetrical single helix along a double station rod. Excerpts from the 700 MHz ¹H NMR spectra (CDCl₃) showing the amide resonances of **2** at 1 mM alone (d, h, l), and in the presence of: **10** (3 equiv, 273 K) after 7 min (e); 30 min (f); and at equilibrium (g); **11** (3 equiv, 273 K) after 7 min (i); 30 min (j); and at equilibrium (k); **12** (3 equiv, 283 K) after 7 min (m); 120 min (n); and at equilibrium (o). Signals of the free single helix, the matching and mismatching complexes on the single station rods are marked with empty diamonds, empty circles and black crosses, respectively. Amide signals of the matching complex at α-station and ω-station, are marked with empty and black circles, respectively.

librium the mismatching complex had disappeared (Figure 3d–g). This indicates that threading through the CC extremity of the helix, that is, threading conducive to the matching complex, has been kinetically favored. In contrast, threading of **11** first produces a majority of mismatching complex that eventually quantitatively converts to the matching complex (Figure 3h–k), confirming the faster threading through the CC extremity, even when it is conducive to a mismatching complex. Additional rods with various termini were prepared (compounds **13–16** in the supporting information). Monitoring foldaxane formation kinetics hints to threading being inherently favored at the CC terminus regardless of the rod functionality (Figures S22–S30). The rate limiting step in the threading process may involve favorable conformations of the helix, desolvation and interactions at the helix entrance. However, there is no information on which of these parameters is critical and why threading may be favored at the CC terminus.

We then prepared **12** to achieve a fully controlled oriented threading. This new rod bears two identical α - and ω -binding stations (Figure 3a) positioned on both sides of a PEG600 spacer. A short *n*-propyl segment before the α -station allows very fast threading/unthreading, while reaching the ω station should be slower. Upon mixing **12** with **2**, NMR showed the immediate and quasi quantitative formation of a new species that corresponds to threading of **2** on the α -station of **12** (**2**⊃**12** α , Figure 3m). No mismatching complex was observed on the α -station presumably because equilibrium was reached before the first NMR measurement. At this early stage, only traces of matching **2**⊃**12** ω could be detected (Figure 3m). Because matching/mismatching equilibrium is reached on the α -station before translation motion to the ω -station occurs, this translation proceeds directly towards the matching **2**⊃**12** ω complex and mismatching complexes are avoided. Of note is the fact that this translation is significantly slower than the formation of for example, **2**⊃**10** (Figure 3n vs. 3f, Figure S30–S31). This slow translation was ascribed to the dissociation of the stable matching **2**⊃**12** α complex. At equilibrium, the proportions of **2**⊃**12** α and **2**⊃**12** ω were similar due to the identical structures of α - and ω -binding stations (Figure 3o). The formation of **2**⊃**12** ω was thus eventually achieved without any detectable level of any mismatching complex, that is, through a fully oriented process.

In summary, this study demonstrates that helical foldamers can be used to design selective molecular recognition patterns of rod-like guests and combine them with fine control of self-assembly kinetics to promote directional sliding processes in which both the rod and the helix have a defined orientation. We showed that a biased threading of a dissymmetrical helix can be programmed by varying the structure of the axle. We also demonstrated that the kinetic segregation of the helix threading and unthreading from its sliding further along the axle made possible a full control over the helix orientation on the rod. Precise anisotropic arrangements as those shown could give access to (poly)foldaxanes with potential use in processive catalysis or transport. Progress in these directions are currently being made in our laboratory and will be reported in due course.

Acknowledgements

This work was supported by the China Scholarship Council (pre-doctoral fellowship to X.W.), the Conseil Régional d'Aquitaine (Q.G.) and by grant ANR-17-CE07-0014. The authors thank Brice Kauffmann (IECB-UMS 3033) for his help during data collection and resolution of the crystal structures. This work has benefited from the facilities and expertise of the Biophysical and Structural Chemistry platform (BPCS) at IECB, CNRS UMS3033, Inserm US001, Bordeaux University.

Conflict of interest

The authors declare no conflict of interest.

Keywords: directional motion · foldamer · foldaxane · molecular recognition · molecular shuttle

How to cite: *Angew. Chem. Int. Ed.* **2019**, *58*, 4205–4209
Angew. Chem. **2019**, *131*, 4249–4253

- [1] For reviews, see: a) S. Erbas-Cakmak, D. A. Leigh, C. T. McTernan, A. L. Nussbaumer, *Chem. Rev.* **2015**, *115*, 10081–10206; b) M. Xue, Y. Yang, X. Chi, X. Yan, F. Huang, *Chem. Rev.* **2015**, *115*, 7398–7501; c) E. R. Kay, D. A. Leigh, F. Zerbetto, *Angew. Chem. Int. Ed.* **2007**, *46*, 72–191; *Angew. Chem.* **2007**, *119*, 72–196.
- [2] For a review, see: “Molecular Machines and Motors”: D. A. Leigh, U. Lewandowska, B. Lewandowski, M. R. Wilson, *Top. Curr. Chem.* **2014**, *354*, 111–138.
- [3] a) C. J. Martin, A. T. L. Lee, R. W. Adams, D. A. Leigh, *J. Am. Chem. Soc.* **2017**, *139*, 11998–12002; b) Y. Qing, S. A. Ionescu, G. S. Pulcu, H. Bayley, *Science* **2018**, *361*, 908–912.
- [4] a) A. B. C. Deutman, C. Monnereau, J. A. A. W. Elemans, G. Ercolani, R. J. M. Nolte, A. E. Rowan, *Science* **2008**, *322*, 1668–1671; b) B. Lewandowski, G. De Bo, J. W. Ward, M. Pappmeyer, S. Kuschel, M. J. Aldegunde, P. M. E. Gramlich, D. Heckmann, S. M. Goldup, D. M. D'Souza, A. E. Fernandes, D. A. Leigh, *Science* **2013**, *339*, 189–193; c) E. M. Peck, W. Liu, G. T. Spence, S. K. Shaw, A. P. Davis, H. Destecroix, B. D. Smith, *J. Am. Chem. Soc.* **2015**, *137*, 8668–8671; d) J. Nishiyama, Y. Makita, N. Kihara, T. Takata, *Chem. Lett.* **2015**, *44*, 1428–1430; e) M. N. Chatterjee, E. R. Kay, D. A. Leigh, *J. Am. Chem. Soc.* **2006**, *128*, 4058–4073.
- [5] a) R. A. Bissell, E. Cordova, A. E. Kaifer, J. F. Stoddart, *Nature* **1994**, *369*, 133–137; b) J.-P. Collin, F. Durola, J. Lux, J.-P. Sauvage, *Angew. Chem. Int. Ed.* **2009**, *48*, 8532–8535; *Angew. Chem.* **2009**, *121*, 8684–8687; c) S. Erbas-Cakmak, S. D. P. Fielden, U. Karaca, D. A. Leigh, C. T. McTernan, D. J. Tetlow, M. R. Wilson, *Science* **2017**, *358*, 340–343; d) A. Goujon, T. Lang, G. Mariani, E. Moulin, G. Fuks, J. Raya, E. Buhler, N. Giuseppone, *J. Am. Chem. Soc.* **2017**, *139*, 14825–14828; e) T. A. Barendt, I. Rašović, M. A. Lebedeva, G. A. Farrow, A. Auty, D. Chekulaev, I. V. Sazanovich, J. A. Weinstein, K. Porfyrakis, P. D. Beer, *J. Am. Chem. Soc.* **2018**, *140*, 1924–1936.
- [6] a) A. Arduini, F. Calzavacca, A. Pochini, A. Secchi, *Chem. Eur. J.* **2003**, *9*, 793–799; b) A. Arduini, F. Ciesa, M. Fragassi, A. Pochini, A. Secchi, *Angew. Chem. Int. Ed.* **2005**, *44*, 278–281; *Angew. Chem.* **2005**, *117*, 282–285; c) A. Arduini, R. Bussolati, A. Credi, G. Faimani, S. Garaudée, A. Pochini, A. Secchi, M. Semeraro, S. Silvi, M. Venturi, *Chem. Eur. J.* **2009**, *15*, 3230–3242; d) A. Arduini, R. Bussolati, A. Credi, S. Monaco, A.

- Secchi, S. Silvi, M. Venturi, *Chem. Eur. J.* **2012**, *18*, 16203–16213; e) A. Arduini, R. Bussolati, A. Credi, A. Secchi, S. Silvi, M. Semeraro, M. Venturi, *J. Am. Chem. Soc.* **2013**, *135*, 9924–9930; f) C. Talotta, C. Gaeta, Z. Qi, C. A. Schalley, P. Neri, *Angew. Chem. Int. Ed.* **2013**, *52*, 7437–7441; *Angew. Chem.* **2013**, *125*, 7585–7589; g) C. Gaeta, C. Talotta, L. Margarucci, A. Casapullo, P. Neri, *J. Org. Chem.* **2013**, *78*, 7627–7638.
- [7] a) T. Oshikiri, Y. Takashima, H. Yamaguchi, A. Harada, *J. Am. Chem. Soc.* **2005**, *127*, 12186–12187; b) Q.-C. Wang, X. Ma, D.-H. Qu, H. Tian, *Chem. Eur. J.* **2006**, *12*, 1088–1096; c) H. Yamaguchi, T. Oshikiri, A. Harada, *J. Phys. Condens. Matter* **2006**, *18*, 1809–1816; d) T. Oshikiri, Y. Takashima, H. Yamaguchi, A. Harada, *Chem. Eur. J.* **2007**, *13*, 7091–7099; e) A. Hashidzume, A. Kuse, T. Oshikiri, S. Adachi, M. Okumura, H. Yamaguchi, A. Harada, *Sci. Rep.* **2018**, *8*, 8950–8958.
- [8] a) T. Nakamura, G. Yamaguchi, T. Nabeshima, *Angew. Chem. Int. Ed.* **2016**, *55*, 9606–9609; *Angew. Chem.* **2016**, *128*, 9758–9761; b) H.-X. Wang, Z. Meng, J.-F. Xiang, Y.-X. Xia, Y. Sun, S.-Z. Hu, H. Chen, J. Yao, C.-F. Chen, *Chem. Sci.* **2016**, *7*, 469–474; c) J.-S. Cui, Q.-K. Ba, H. Ke, A. Valkonen, K. Rissanen, W. Jiang, *Angew. Chem. Int. Ed.* **2018**, *57*, 7809–7814; *Angew. Chem.* **2018**, *130*, 7935–7940; d) S. Varghese, P. B. White, J. A. A. W. Elemans, B. Spierenburg, R. J. M. Nolte, *Chem. Commun.* **2018**, *54*, 12491–12494.
- [9] a) M. Guix, S. M. Weiz, O. G. Schmidt, M. Medina-Sánchez, *Part. Part. Syst. Charact.* **2018**, *35*, 1700382; b) T.-C. Lee, M. Alarcón-Correa, C. Miksh, K. Hahn, J. G. Gibbs, P. Fischer, *Nano Lett.* **2014**, *14*, 2407–2412.
- [10] Y. Ferrand, I. Huc, *Acc. Chem. Res.* **2018**, *51*, 970–977.
- [11] a) Q. Gan, Y. Ferrand, C. Bao, B. Kauffmann, A. Grélard, H. Jiang, I. Huc, *Science* **2011**, *331*, 1172–1175; b) Y. Ferrand, Q. Gan, B. Kauffmann, H. Jiang, I. Huc, *Angew. Chem. Int. Ed.* **2011**, *50*, 7572–7575; *Angew. Chem.* **2011**, *123*, 7714–7717; c) Q. Gan, Y. Ferrand, N. Chandramouli, B. Kauffmann, C. Aube, D. Dubreuil, I. Huc, *J. Am. Chem. Soc.* **2012**, *134*, 15656–15659; d) S. A. Denisov, Q. Gan, X. Wang, L. Scarpantonio, Y. Ferrand, B. Kauffmann, G. Jonusauskas, I. Huc, N. D. McClenaghan, *Angew. Chem. Int. Ed.* **2016**, *55*, 1328–1333; *Angew. Chem.* **2016**, *128*, 1350–1355.
- [12] X. Wang, B. Wicher, Y. Ferrand, I. Huc, *J. Am. Chem. Soc.* **2017**, *139*, 9350–9358.
- [13] Y. Ferrand, A. M. Kendhale, J. Garric, B. Kauffmann, I. Huc, *Angew. Chem. Int. Ed.* **2010**, *49*, 1778–1781; *Angew. Chem.* **2010**, *122*, 1822–1825.
- [14] Q. Gan, X. Wang, B. Kauffmann, F. Rosu, Y. Ferrand, I. Huc, *Nat. Nanotechnol.* **2017**, *12*, 447–452.

Manuscript received: November 16, 2018

Accepted manuscript online: January 16, 2019

Version of record online: February 20, 2019